Article:
Buswell, R., Xu, J., De Becker, D. et al. (4 more authors) (2022) Geometric quality assurance for 3D concrete printing and hybrid construction manufacturing using a standardised test part for benchmarking capability. Cement and Concrete Research, 156. 106773. ISSN 0008-8846

https://doi.org/10.1016/j.cemconres.2022.106773

Cement and Concrete Research 156 (2022) 106773

Contents lists available at ScienceDirect

Cement and Concrete Research

journal homepage: www.elsevier.com/locate/cemconres

Geometric quality assurance for 3D concrete printing and hybrid construction manufacturing using a standardised test part for benchmarking capability

Richard Buswell [a], Jie Xu [a,*], Daniel De Becker [a], James Dobrzanski [a], John Provis [b], John Temitope Kolawole [a], Peter Kinnell [c]

[a] School of Architecture, Building and Civil Engineering, Loughborough University, Loughborough, UK
[b] Department of Materials Science and Engineering, The University of Sheffield, Sheffield, UK
[c] Wolfson School of Mechanical Electrical and Manufacturing Engineering, Loughborough University, Loughborough, UK

ARTICLE INFO

Keywords:
3D Concrete Printing
Hybrid concrete printing
Manufacturing tolerance
Geometric conformance
Quality control and assurance

ABSTRACT

The need for quality control and assurance in 3D Concrete Printing (3DCP) is widely recognised. Achieving geometric accuracy to a specified tolerance is a cornerstone of component-based production and assembly. Although published work within the field recognises such issues, these fall short of proposing systematic methods to evaluate, diagnose, improve, monitor and compare system performance. This work takes inspiration from the test geometry approach readily deployed in Additive Manufacturing and develops a full-scale test part to establish a reproducible benchmark for evaluating and assuring part geometric quality of 3DCP systems. The approach is used to evaluate the benefits of a new fabrication approach that combines subtractive milling on green cement mortar in combination with 3DCP. It was demonstrated to yield useful information for direct comparison of different processes and diagnosing problems for performance improvement. The test part and measurement approach offer the 3DCP community a means of cross-platform benchmarking of 3DCP system performance.

1. Introduction

Over the past 15 to 20 years, 3D Concrete Printing (3DCP) has become established as one of the principal new technologies within the wider field of Digital Fabrication with Concrete (DFC) [1]. It is rapidly developing in terms of the scale, volume and variety of applications for either off-site manufacture or as part of the construction process on-site [2]. The methods are based on the principles of Additive Manufacturing (AM), where an accurate digital model of the part geometry (the net-shape) is processed directly, 'sliced', to produce a series of layers which are sent to a machine that selectively places, solidifies, or binds material in sequential layers to produce a close approximation to the net-shape geometry [3]. In construction, cement-based mortars are used most commonly through a material extrusion approach, where fresh material is pumped to create a continuous filament and typically positioned using CNC-controlled robotic arms or gantry systems.

Although the capabilities of manufacturing have been demonstrated in terms of scale, these are still largely through demonstration projects where the accuracy and precision in achieving the net-shape geometry is less well understood. Many groups are now beginning to measure printed components to assess the accuracy and defects in printing, recent examples of which are [4–9]. The resultant geometry of a printed part is affected by a number of issues including plastic deformation [10], the 'staircase effect' at the surface [11] and shrinkage [12]. The influence of the positioning system used in the deposition process on part accuracy is less well understood, although there is growing awareness of positioning errors and movement in the light-weight systems that are commonly deployed. Currently, there are no published methods that can assist in the systematic evaluation of these errors to underpin testing, evaluating and benchmarking performance.

Concurrently, new methods for treating known imperfections, particularly surface finish, through secondary processes, applied after printing are under development through trowelling and milling [13–16]. These hybrid methods offer new possibilities for surface quality/finish, and manufacture accuracy and precision, however, there are no methods with which to systematically assess the benefits, or to

* Corresponding author.
E-mail address: j.xu2@lboro.ac.uk (J. Xu).

https://doi.org/10.1016/j.cemconres.2022.106773
Received 9 December 2021; Received in revised form 10 March 2022; Accepted 10 March 2022
Available online 1 April 2022

benchmark capability improvements on one system, or compare the capabilities of one system with those of another.

The work reported here takes inspiration from the test geometries commonly found to assess the capabilities of mainstream Additive Manufacturing [17–24] and develops a new test geometry tailored for 3DCP and associated hybrid 3DCP approaches. To inform the design of the test part, a state-of-art review of geometric formation in 3DCP was undertaken, and a selection of features and errors informed through Geometric Dimensioning and Tolerancing (GD&T) methods was applied to create a formal approach to geometrical assessment through a repeatable and platform-independent test.

The approach is then used to evaluate the benefits of a hybrid process over 3DCP only manufacture. The former uses an inflated model of the net-shape for printing, and then applies milling to trim the surface back to the net-shape, the latter uses a 3DCP tool path sized to achieve the net-shape. A realistic 'print first time' approach was taken, and the approach was shown to be able to evaluate the differences at scale, and, in particular, its ability to highlight systematic errors in code production through the digital translation from CAD to machine instructions as well as unseen errors in the positioning system. Approaches such as this are critical at debugging the software and mechanical systems in addition to evaluating the performance of the material during printing. The test geometry developed is freely available to download [25], in the hope that others will deploy it to evaluate their systems.

2. Background to 3DCP and geometry reproduction

There are many well-known advantages of manufacturing additively, which include affordable and flexible production runs, customisation for free, efficient use of material and the elimination of tooling [26]. The removal of the need for moulds enables the realisation of directed digital control of the manufacturing process, delivering the foreseen benefits. Some of the gains in time and resource use in the pre-production steps, however, are mitigated by the need for post-processing operations, such as extraction of the part from the manufacturing equipment, trimming, cleaning and finishing [3]. The finishing, dimensional precision and geometric accuracy can influence the Technology Readiness Level of such technologies [27–29].

Of key interest in Additive Manufacturing is the ability to recreate features, and so printing resolution and minimum feature size has, and still is, of considerable interest in defining the capability of processes. In order to evaluate these, there have been a host of test parts developed to explore different processes and the reproduction of different features, Fig. 1 shows a few. The test part in Fig. 1a is one of the first test artefacts designed to quantify the manufacturing precision (focusing on the x-y plane) of Stereolithography (SLA) processes. Mahesh et al. [18] developed a test part (Fig. 1b) of 170 mm × 170 mm with comprehensive geometric features (e.g., holes, slots, walls, columns, slopes) and overhangs for Rapid Prototyping systems. The test artefact in Fig. 1c, developed at the National Institute of Standards and Technology of US, had a height of 17 mm and a volume of approx. 101,000 mm^3, with 4 mm pins and holes aligned along the x- and y-axes and diamond-shape lateral features (for easy upright mounting for measurement). These benchmark parts are all designed with reference to GD&T and/or ISO standards.

The same challenges are also true for the larger scale processes that can be found in construction and architecture, although the importance of features have a different scale, which maybe one or two orders of magnitude larger than that in consumer products and aero/automotive industries. In order to identify the geometries and features that are of importance in contemporary 3DCP manufacture, a literature review was undertaken in August 2021 using Google Scholar. The keywords used were 'concrete printing', successively combined with various geometric-related keywords, such as: 'accuracy', 'precision', 'surface finish', 'surface quality', 'geometric constraints', 'shape complexity', 'form complexity', 'cantilever/overhang', 'doubly curved', 'hollowed' and 'multifunctionality'.

From the early work in 2011 [11], the increase over the last four years has seen a nearly seven-fold, from a total of six articles in 2017, to over 40 in 2021. Of those, 24 relate to material extrusion and jetting based 3DCP, and of these 75% related to geometric complexity, exploring forming limitations or demonstrating the ability to achieve some forms. 58% dealt with the geometric conformity, the capability of the process to achieve the net-shape and surface finish. Eight papers included both aspects.

The data from those 24 papers was extracted and is presented in Table 1, which provides an overview of application categories manufactured using 3DCP. There are three scales/types of products: single components, assembled structures and surface textures. For each article of interest, Table 1 provides the application, scale of component and the potential geometrical features of interest, based on GD&T principles [4]. Those that reported an assessment of geometric conformity are summarized in Appendix A, Table A.1 and Table A.2, suggesting that errors from 3DCP alone can be of the order of ±20 mm, although the numbers of examples are very small and insufficient for generalised conclusions. In general, these works are focused on a platform-dependent reproduction of a component unique to that study and so comparison of process capability, or benchmarking performance is practically impossible.

The deformation of the material during printing and the surface effect created by layering may be improved, but are likely to remain challenging, and may prove to prohibit the routine application of 3DCP components in some applications: ones where interfaces are required with other building systems, for example [30]. Individual manufacturing processes have been shown to have drawbacks in producing various components in terms of form-freedom, waste and strength [31–33]. It is likely, therefore, hybrid processes [1,34] that take advantage of the flexibility of 3DCP, with additional accuracy, precision and surface finishing options will become more popular.

The tools, methods and procedures needed to systematically benchmark performance in order to evaluate, diagnose, improve, monitor and compare system performance are required to advance the

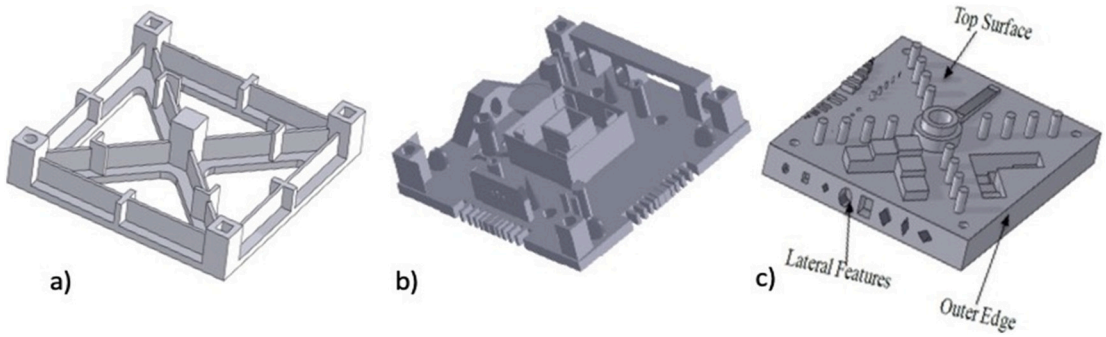

Fig. 1. Test part geometries to explore reproduction capability in Additive Manufacturing: a) from [17], b) from [18], and c) from [23].

Table 1
Overview of 3DCP product categories in the subsampled literature.

Application		Form (feature)	Scale (L: length, H: height, W: width)	Possible interested geometric tolerance	Reference	Product number
Single components	Wall & column	2.5D (curved or flat side surface)	Not given	Perpendicularity of side face and edge;	[35]	1
			D 0.5 m *H 400 mm	Profile (cylindricity) or flatness of side	[10]	2
			Not given	face;	[15]	3
			Not given	Straightness and angularity of edge	[36]	4
		3D cantilever (max inclination from vertical: 30°)	D (0.4–1.2) m * H 1 m	Profile of side face	[14]	5
			L 2.5 m * W 0.18 m * H 2.3 m		[6]	6
			Not given		[36]	7
			D (0.4–0.8) m * H 2.75 m		[9]	8
	Dome / vault (shell)	3D cantilever (max inclination from vertical: 90°) / Doubly-curved	D 14.6 m * H 3.7 m	Profile of side face	[37]	9
			L 1 m * W 0.5 m* H 0.2 m		[38]	10
	Cladding panel	Doubly-curved (max inclination from horizontal: 30°)	0.75 m * 0.75 m * 24 mm	Profile and parallelism of side face;	[39]	11
			≤ 1.2 m * 1.2 m * 30 mm	Angularity of edge	[40]	12
			1 m * 1 m		[41]	13
			0.21 m * 0.21 m * 10 mm		[42]	14
	Volumetric part (test specimen)	Star shape	D 0.5 m *H 200 mm	Flatness and angularity of flat surface	[11]	15
		Polyhedron, domes / vaults, etc.	L 430 mm * W 400 mm * H 100 mm	Profile, flatness and angularity of side face	[4]	16
			H 90 mm		[7]	17
			H 210 mm		[7]	18
			H 225 mm		[7]	19
			H 225 mm * L 1 m * W 180 mm		[8]	20
Assembled structures	Pavilion (volumetric)	Consisting of 47 unique parts	D 6.2 m * H 2.7 m	Profile of curved surface;	[43]	21
	Pavilion (shell)	Consisting of 110 unique parts	L 12 m * W 5 m * H 3 m	Profile, position and flatness of jointing face	[44]	22
Surface textures		Inclined surface/tapering	Inclination: 0–90°	Position, profile and angularity of any individual features	[13]	23
		Holes/slots;	Hole diameter: ≤ 200 mm;		[15]	24
		Carved pattern	Pattern width: ≥ 3 mm		[36]	25
		Raised pattern	Pattern width: ≥ 9 mm		[45]	26

geometric quality in the reproduction of parts from using 3DCP and hybrid manufacturing systems.

3. Designing the test part and evaluation procedure

The literature summarised in Table 1 highlights two of the most common applications for 3DCP, the production of walls printed vertically (large length, small width, large height) and panels printed horizontally (large length, large width, small height). Both these applications drive the process to print in two modes: 1) homogeneous 'as good as cast' mode, often required for panel production [39–42]; and 'vertical shell' mode commonly used for the production of walls and columns, but also applied for printing formwork and for the production of many volumetric objects such as street furniture [6,9,43,46,47]. The shape of these may include straight or curved edges and vertices. Other features may be desirable such as cantilevers, rebates, or occlusions that might form desirable features.

The test part should reproduce these features at a scale directly relevant to reality and it should also be applicable for as broad range of 3DCP and hybrid processes as possible. In an ideal situation, the material volume would be minimal and the geometry fairly straightforward to encode, manufacture and to measure: although at the current stage of development, the focus here is on the geometry. Table 2 lists a useful subset of these features together and Fig. 2 depicts an interpretation of these features into a single part test geometry of 1 m by 1 m by 1 m (dimensions b, c and d in Fig. 2).

Because the evaluation is based on the end-to-end production, from CAD geometry to physical component, all potential errors are captured: through the translation from CAD to toolpath with the set-up of tooling, the translation of toolpath to absolute positions in the build volume, through deformation of the wet material and pump rate/deposition volume mismatch, and any shrinkage. Hence, using the geometry not only benchmarks the process, but also yields very rich diagnosis data which allows the improvement of process performance. This is assisted through the inclusion of planar surfaces, which are geometrically (and mentally) easier to visualise when undertaking diagnosis. The inclusion of 90° vertices are very practical for interfacing with other construction systems, they are simple to evaluate and are challenging to reproduce using 3DCP.

Table 2
Dimensions, geometric characteristics and surface finishes of the test geometry.

Category	Section/feature	Interested item
Dimensions	Wall	Length
		Width (thickness)
		Height
	Panel	Length
		Depth (thickness)
	Rib	Width (thickness)
		Height
Geometric characteristics	Panel rebate	Depth
		Width
	Wall sides	Perpendicularity to base / between adjacent ones
	Chamfer top	Angularity (from horizontal)
	Panel hole	Radius
		Position of centre
	Panel fillet	Radius
	Rib fillets	Radius
Surface finishes	Wall	Front / back / left / right / top faces
	Panel	Top face

System performance and quality checks can be undertaken at one of four stages in a manufacturing process: 1) pre-manufacturing as part of system commissioning, setting to work and monitoring; 2) during manufacturing, as part of pre-print checks, that might consider material, systems, software and code implementations and curing environment; 3) post manufacture, verifying the product meets its specification; and 4) in some cases, post-installation where a component is monitored through

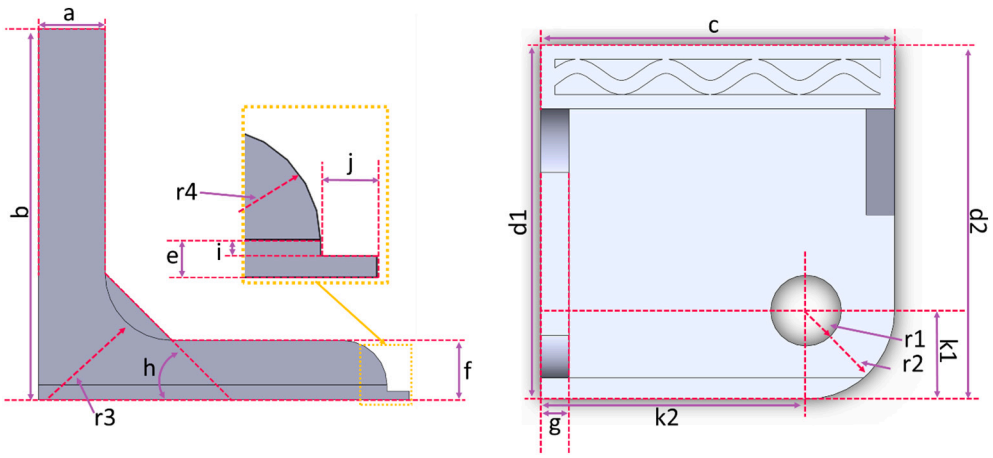

Fig. 2. The standard test geometry depicting features and measurement locations.

its service life. This work focuses on the pre-manufacturing phase and can be used in commissioning/verification, periodic monitoring and systems checking, and for the calibration of two independent systems so that they manufacture to the same tolerances.

3.1. Evaluation procedure

Evaluation of the manufacturing process is required for both printed and milled part validation, consisting of a systematic assessment of the manufactured component. The approach was split into a two-step process and has been made generic to allow for the measurements to be made using any available equipment and software.

3.1.1. Initial visual inspections

The initial visual inspection allows for any obvious errors or flaws to be observed. This is primarily a qualitative analysis of the component, where simple images are captured with an associated description of the error and the probable causes of this error. This allows for any evident errors within the test geometry to be considered during the quantitative analysis. These errors are listed and, their causes or potential causes are noted in a comprehensive manner. These form the bases of a systematic error checking and diagnoses, which may be correctable (human error) or could be part of the CAD-to-Part implementation chain: software, control, mechanical systems, material, etc.

3.1.2. Obtaining measurement data of test geometry

The second step is to evaluate the dimensional precison and geometric accuracy of the test part and thus determine the overall accuracy of the manufacturing system. To support this, the 17 features illustrated in Fig. 2 are suggested for measurement using the nominal dimensions in Table 3.

4. The case specific details

The Standardised Test Part approach (termed here as STP method) was used to evaluate the geometric accuracy and precision benefits offered by adding a subtractive process to an extrusion based 3DCP. The equipment has been used for 3DCP for some time and has been upgraded to undertake hybrid operations (milling in this case). The milling equipment and process on green mortar has been tested and validated independently [16] and now the system is ready to implement the full hybrid process to establish:

1) at which error level (min. tolerances or max. accuracy) the end-to-end, CAD-to-Part process (hardware, software, material) works;

Table 3
Description and expected values of the measurements.

Description	Label	Expected value
Wall thickness	a	180 mm
Wall height	b	1000 mm
Wall length	c	1000 mm
Panel length	d	1000 mm
Panel thickness	e	40 mm
Rib height	f	160 mm
Rib width	g	80 mm
Chamfer angle	h	45°
Rebate depth	i	17 mm
Rebate width	j	60 mm
Hole radius	r1	100 mm
Panel fillet	r2	250 mm
Wall-to-rib fillet	r3	180 mm
Rib-to-panel fillet	r4	120 mm

2) the improvement in part accuracy and precision afforded by the addition of the milling process; and,
3) the comparison of the overhead in production time for both approaches.

4.1. The 3DCP and hybrid systems

The system apparatus is presented in Fig. 3. It comprises an ABB IRB 6640 6-axis robotic arm with a 2.4 (L) * 1.5 (W) m^2 high-precision aluminium turntable mounted on an ABB MID 1000 Rotary Unit. The arm reach is up to 2.55 m and has a payload of 180 kg. A preblended mix is fed from m-tec Piccolo Silo, which supplied a m-tec D10 inline mixer. Admixtures can be dosed with water at the entry to this. The mixture is discharged into a m-tec P20 worm pump for conveying to the Concrenetics 'One-X' dynamic mixing head mounted at the end of the robotic arm. The system allows for dosing the mortar with admixtures prior to deposition through a Ø20 mm circular nozzle.

The subtractive tooling can be interchanged with the printing head utilising the same robotic arm. It comprises of an ELTE srl AF110 spindle motor and a 12 mm diameter, 283 mm long, 2-flute ball nosed cutter, which can be deployed to cut either at the tip, or along the shank of the tool if the set of the mortar is in a sufficient early stage [16]. The cutter can operate up to 2000 rpm.

4.2. Material control

The mortar for printing consists of a preblended dry (powder) materials of Portland cement (CEM I), fly ash, silica fume with binder

Fig. 3. a) The robotic arm set up for printing (continuous mixing, right-hand side) and measurement (left-hand side), and b) set up for milling.

percentages of 70%, 20% and 10% respectively and sand (<2 mm) formulated for high performance concrete. Details of the formulation and applications can be found elsewhere [16,48,49]. The liquid contents (water, MBCC MasterGlenium SKY 1966 superplasticiser, and MasterSure 1970 consistency retainer) were injected into the D10 continuous mixer at controlled flow rates (expressed in mass constituents as shown Table 4-1) based on the pre-established powder flow rate.

Due to a limited 15-second residency time of the continuous mixer, the open time [48] was not achievable and a modified formulation outlined in Table 4-2 was used to increase the open time to ten hours. MBCC MasterRoc SA194 aluminium sulphate-based accelerator was injected at the printing head and dynamically mixed to match the pumped concrete flow rate of 3.2 kg/min, which created the set-on-demand concrete with the required printability and buildability. The pre-determined content of the accelerator and obtained rheological properties [50,51] is shown in Table 4.

4.3. Digital workflow and toolpath preparation

The solid model of the test part is sliced and the toolpaths were configured in a conventional manner common to most 3DCP approaches. The pink and red sections in Fig. 4 depict this and the resultant print and then measurement for evaluation. In this case, the toolpaths are designed to produce the outer edge of the deposited filament as 'dead-size' for the solid model, the desired net-shape. The hybrid approach carried out the same operations, but on a net-shape that is inflated by 10 mm globally, so the resultant print of over-sized by about half a filament width, seen in Fig. 5. A second set of toolpaths is generated that guide the milling operations (the green shaded sections of Fig. 4), that cut the inflated part back to the net-shape. These are applied after the printing while the mortar remains in a green state, at which point measurements can be taken.

In this work, Autodesk PowerMill was used to generate the toolpaths. The inclusion of the milling brings additional tooling management overhead, requiring preselection of tools, stepover, feed rates and milling strategies. Once complete, simulations are run with the software to identify any collision issues and then the robot performs a 'dry run' to identify any potential part collisions prior to manufacturing with the physical equipment. For this part (1 m^3), milling is required on all sides and hence it is not possible to complete without rotating the part, see Fig. 6.

Table 4
Modified mix for the two-component high-performance set-on-demand 3DCP.

4-1: Material composition (informing flow rate)				
Printed concrete	Pumped concrete	Pre-blended dry materials (kg/m^3)		2074
		Water	Water/binder ratio	0.26
			Content (kg/m^3)	212
		Superplasticiser (kg/m^3)		18.26
		Consistency retainer (kg/m^3)		1.66
	Accelerator (kg/m^3)			50

4-2: Target fresh properties		
Pumped concrete	Yield stress (Pa)	200
	Plastic viscosity (Pa·s)	26.6
Printed concrete	Structuration rate (Pa/s)	200

4.4. The measurement system

A customised structured light measurement system designed for large-scale components was set up to be capable of a measuring range between 1.5 and 4.0 m, details in Table 5. It was mounted on an adjacent ABB IRB 6640 robot (Fig. 4a, left-hand side) that allowed convenient positioning in the manufacturing cell.

Calibration was carried out with a 1080 mm by 810 mm calibration board with black-white grids. The calibration process involves taking images of the calibration checkerboard at various angles and distances to the image sensor planes. The calibration estimates the mean error of all points used during the calibration, which is used to estimate the accuracy of the scanner. In this work, the mean error of calibration points was 60 μm, with standard deviation of 130 μm, which gives an expected point uncertainty of 0.45 mm, for a coverage factor of three.

Twenty overlapping scans were taken, each generating a point cloud, which were amalgamated into a single 3D representation of the manufactured part. To measure the test part, the scanner was positioned adjacent to the part and the part could be rotated using the turntable. To capture all aspects of the object, the turntable was rotated 30 degrees azimuth, with the camera system set at an altitude (zenith) angle of 45 degrees relative to the part. Scans were taken at two heights, 1 m and 2 m over the workpiece during the scanning process, which ensured complete coverage of the sides and top of the object. To validate this process and assess the expected accuracy of the resulting point cloud, a calibrated ball bar was positioned in the measurement frame of the part, so that it was visible in multiple scans. The ball bar consisted of the 19 mm diameter spheres mounted to a calibrated rod, such that the distance

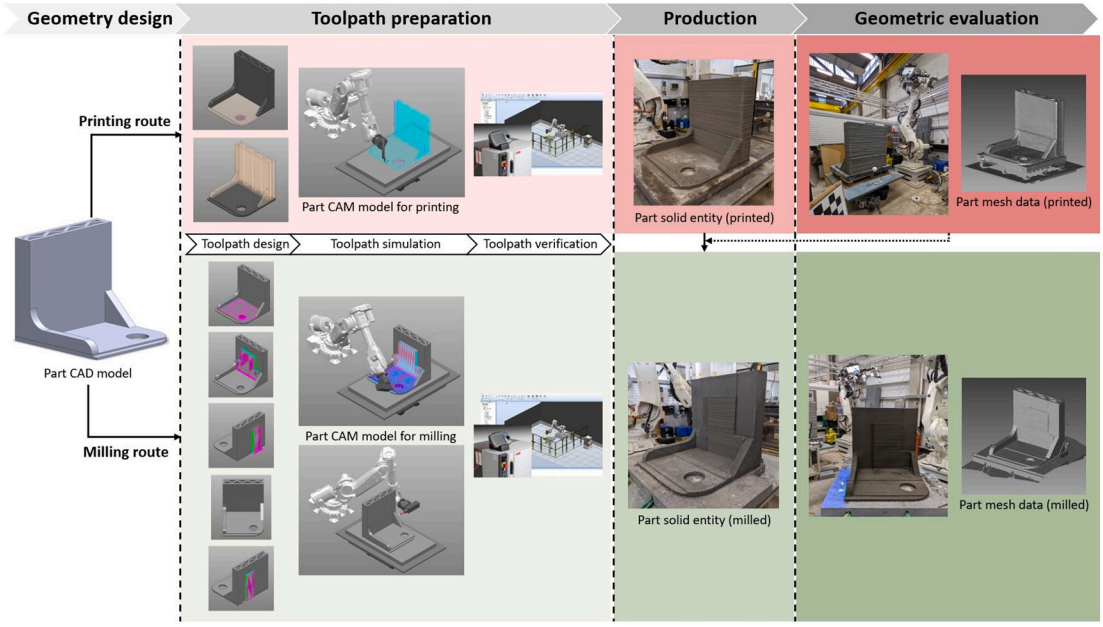

Fig. 4. CAD-to-Part workflow for 3DCP only (on the top row) and the subtractive milling (on the bottom row).

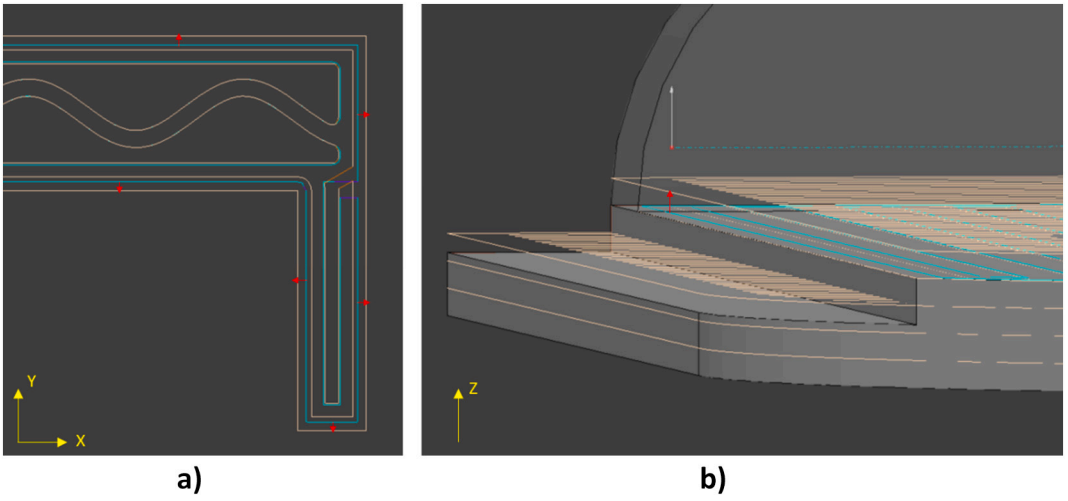

Fig. 5. Inflation of the printing paths in a) the horizontal direction - top view of the wall-chamfer junction, and b) the vertical direction - 3D view of the panel rebate (cyan: original 3DCP printing path; brown: inflated printing path).

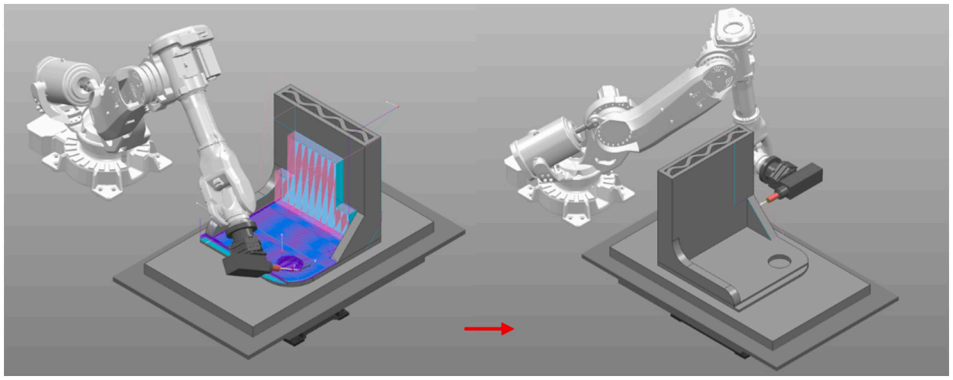

Fig. 6. Simulation of the milling paths demonstrating that the part needs to be rotated by 90° degrees so that the robot can reach and mill the far side of the part.

Table 5
Specifications of the customised measurement system.

Component		Specifications
Structured light scanner	Projector	CASIO XJ-F100W f2.5, 3500 lm
	Dual camera	12 mega-pixel Basler L acA4096-30 um, using 16 mm lenses
	Mini PC	Intel NUC Gen 8 i7
Scanning software		Polyga FlexScan3D

between sphere centres was 500.225 mm. By fitting spheres to the points in the amalgamated point cloud that represented the two spheres, the largest distance was measured as 500.935 mm, resulting in an error of 0.709 mm.

The fused point cloud provides data over the whole areas of the part (Fig. 7a), as opposed to a sampled measurement achieved using a tape measure, and can be used for calculating maximum/minimum (Fig. 7b) and mean (Fig. 7c) dimensions as well as measures of surface finish. CloudCompare software [52] was used to fit a best-fit plane to a reference plane, and then the positions of points on opposing faces are projected onto the reference, each providing a distance measurement. There are 130 points per 10 mm^2 of surface area and so all features are captured down to a resolution of 0.07 mm^2 per point. To account for deviation across the plane, that is due to the uneven nature of the finished surface plus any form deviations from the target flat plane surface, the mean plane fit is considered along with three standard deviation limits to define the maximum positive and negative perpendicular projected distances of measured surface points from the mean fit plane.

5. Results

5.1. Process set up and implementation

The case study was set up in a realistic, 'print a new part first time' approach. The equipment has been successfully used prior to this work for the production of large panel systems (e.g. 400 kg panels). The milling system for mortar in its green state was developed focusing on the approach taken for producing the test part, reported in [16].

Apart from a small 'test of principles' print, the Standard Test Part method (or STP method, named so here) would test the build rate and static yield stress control required to print a vertical wall section in reasonable time. This was also the first time the test geometry described in this paper was manufactured and the first time the milling had been applied to a large surface area. The reporting here has intentionally been kept honest and open, as implementing these systems is complex and representative of many if not all 'first-time' trials. For others wishing to implement the test geometry to test their machines, this also gives representative guidance on what outcomes to expect.

5.2. Printing and milling operations

The whole production (printing and milling) process was operated on a piece of rigid foam placed on top of the turntable until completion; the use of the foam as a base material was for safely holding the mill cutter when milling the edge of the bottom panel. The overall production speed and timing details are presented in Table 6. The inflation in the printing paths used in the hybrid (H-3DCP) process has led to an approximate 50% increase in the printing time.

Two parts were manufactured on two separate days. The hybrid process required tool change over on the end of the robotic arm after printing and as can be seen from Table 6, the manufacturing time for the hybrid part took about 7.5 hours as opposed to 1.5 hours for the purely printed component.

5.3. Quality control stage 1: visual inspection

Fig. 8 illustrates the subjective differences between the 3DCP part (top) and the hybrid part (bottom). Observable issues with the 3DCP part include: a) over-printing across the width of the wall, which was attributed to a coding error resulting in a layer being double printed (subsequently corrected for the hybrid part); and b) over-printing at edges and features which is due to the relative mismatch between the deposition volumetric flow rate and the robot travel speed as the robot slows down to change direction, exacerbated by relatively small feature sizes (with respect to the nozzle diameter). The known staircase effect can be clearly seen, limiting the resolution of straight and curved feature replication.

The over-printing issues are largely negated by the milling and the formation of edges and flatness of surfaces are improved by a significant extent, as are the replication of the rebate and curved features. However, the milling operations were not without error. The most significant was in relation to the mismatching of absolute tool position when a) different robot joint configurations were utilized to reach the same position, and b) when the part was rotated on the turntable. These issues occur when the whole part has to be milled in different azimuths where the robot

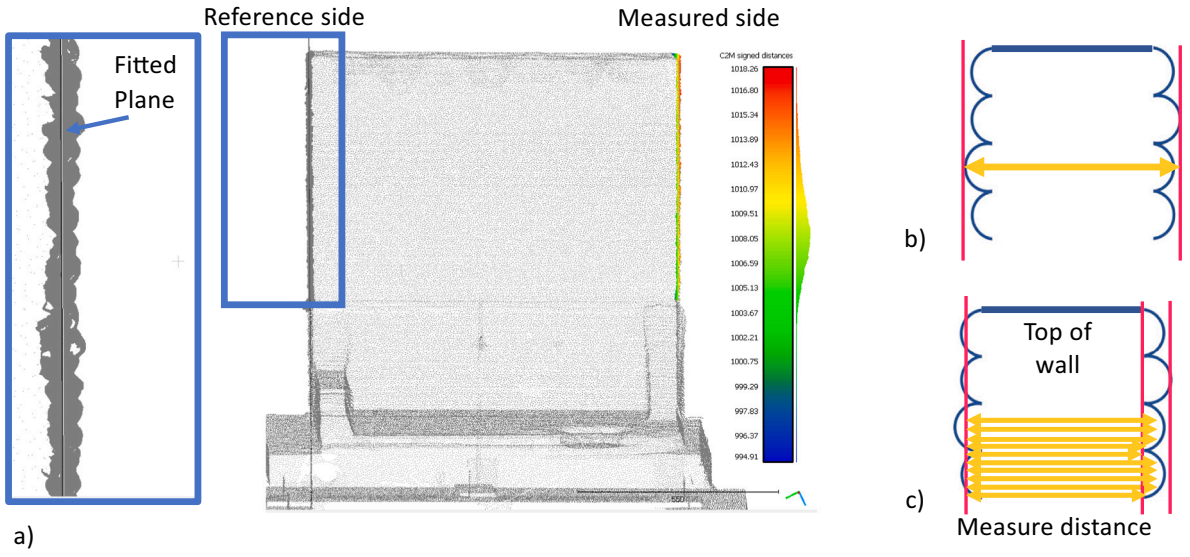

Fig. 7. Measurement approach showing the identification of mean surface and deviation measurements.

Table 6
Production speed and timing details.

	Setup time [min]	Volume flow rate [ml/min]	Printing speed [mm/s]	Printing time [min]	Downtime [min]	Milling speed [mm/s]	Milling time [min]
3DCP	~ 30	1800	150	~ 95			
H-3DCP	~ 30	1410 (for rib-chamfer-wall) 1800 (for panel)	150	~ 140	~ 120	50 (@ 1500 RPM)	~ 200

Fig. 8. The 3DCP part (top) and the hybrid part (bottom) inspection images.

Table 7
Hand and tape measurements to the nearest mm of both printed and milled parts. Labels and description relate to the dimensions given in Fig. 2. 3DCP estimates are with an uncertainty of ±3 mm to ±5 mm, and hybrid (H-3DCP) less than ±2 mm.

	Description	Target (mm)	3DCP Error Min (mm)	3DCP Error Max (mm)	H-3DCP Error Min (mm)	H-3DCP Error Max (mm)
A	Wall thickness	180	-15	6	0	2
B	Wall height	1000	4	10	3	9
C	Wall length	1000	10	25	-	-2
D1	Panel length (LHS)	1000	10	20	-	9
D2	Panel length (RHS)	1000	0	14	-	7
E	Panel thickness	40	-	10	-	0
F	Rib height	160	-	1	-	0
G	Rib width	80	0	10	-	0
I	Rebate depth	17	-1	7	-	-2
J	Rebate width	60	-	-3	-	0
K1	Hole position	250	-	5	-2	-2
K2	Hole position	250	-	5	-	-1
M	Hole diameter	200	20	30	-2	1

joints are in significantly different positions, or the relative position between the robotic arm and the turntable are slightly out of alignment which results in a stepping on an otherwise flat surface. The error in the misaligned turntable under rotation was significant causing an 8 mm step in the surface, clearly identifying the need for greater calibration of the positioning system.

Table 7 gives a series of hand measurements over the linear distances of the part, using a sample. The uncertainty in these measurements was estimated to be in the range of ±3 mm to ±5 mm on the 3DCP part and less than ±2 mm on the milled part, using a hand-held tape measure. For the linear dimensional measurements on the printed part, notional minimum and maximum estimates were made, by eye. The results are quite striking in that the milled part is far more consistent in dimensional accuracy and has more precise surfaces, which might be expected as the shaping is carried out on solid material: rheology is no longer a factor.

There are some dimensions that are worse than anticipated, such as the wall height: here the milled part was inflated, but the top of the panel was not milled back (an error in production) and so the +9 mm represents the oversized printing (+10 mm in the inflated model). In addition, during printing, a reasoned conclusion might be that better control and precision of extruded filament width would improve the accuracy of the printed part. Panel length does appear to have some error in both parts, which might be attributed to a systematic positioning error in the robotic arm, since the tool-path codes were different in each case. However, with the hybrid system errors resolved, the data would suggest that an order of magnitude better manufacturing accuracy might be expected with the application of the secondary milling over the pure 3DCP part, even if control of the printing process was improved.

5.4. Quality control stage 2: digital measurement

The digital measurements are split into three categories: linear dimensions; surface flatness; and feature replication. The linear measurements align with the hand-tape measurements, except they are informed by the entire surface of interest and so are more complete, measured to a higher degree of accuracy and can be adapted more readily to the evaluation of non-linear/planar features. Table 8 details the mean and maximum dimensions for the linear measurements detailed in Fig. 2 using the point cloud data captured by the structured light scanner. The 95% confidence limits on the estimates of the mean distances are in the order of 1.0 μm, and so the standard deviation is reported as this provides more information regarding the precision of the surface used to generate the mean value.

The angles achieved were assessed by fitting planes to the surface and then calculating the angels between these planes (for example, the 90° edges on the wall and the 45° chamfer: measurement 'h' in Fig. 2) and these were all found to be excellent: between −1.8° and +1.4° for the 3DCP part and between −0.3° and +0.3° for the hybrid part. Not surprisingly, there was a significant improvement on surface flatness when the milling was used as can be seen in the standard deviations reported in Table 8, better than an order of magnitude improvement. The digitally augmented comparison of the difference between 3DCP and hybrid is shown in the third image from the left in Fig. 9, which reflects the part photographs in Fig. 2. The other features are also given to present the digitally augmented inspection, with a common colour scale to show error. The milled surfaces are clearly superior to the printed for the fillet, radius and circular hole formation. The under printed area (blue) in the bottom left image (milled fillet) was due to a layer approximation error: although the part was inflated, the staircase approximation left this under printed: which demonstrates the power of replicating known features in order to test and diagnose problems in the production workflow from design for manufacture, through toolpath generation to machine operation.

6. Discussion

The development of 3DCP is reaching landmark levels [2] and increasingly hybrid processes are being developed for quality benefits [13–16]. The maturity of the technology is such that full scale research can be undertaken alongside commercial systems for sale to deliver construction scale applications [30,53,54]. The need for quality control and assurance is growing and recognised for wet and hardened materials [55,56] and this work offers the first systematic approach to quality checking and assurance for the geometric accuracy and dimensional precision of parts manufactured using 3DCP and hybrid methods.

The principal idea behind the approach is that a carefully designed part of known dimensions can be replicated on any 3DCP or hybrid

Table 8
Structured light and point-cloud based measurements of the linear dimensions, to the nearest mm of both printed and milled parts. Labels and description relate to the dimensions given in Table 3. The measurement precision for both cases is within ±0.7 mm. Mean and maximum measurements are given where 'Maximum' is defined as (approximately) 1% point inclusion, determined to be +3 mm standard deviations on mean.

	Description	Target (mm)	H-3DCP Stdev. surface (mm)	3DCP Error mean (mm)	3DCP Error max (mm)	H-3DCP Stdev. surface (mm)	H-3DCP Error mean (mm)	H-3DCP Error max (mm)
A	Wall thickness	180	1.06	3	9	0.16	3	4
B	Wall height	1000	0.35	3	8	0.23	1	10
C	Wall length	1000	2.65	6	22	0.21	-4	-2
D1	Panel length	1000	1.06	1	14	0.3	9	11
D2	Panel length	1000	1.25	10	12	0.41	9	11
E	Panel thickness	40	0.35	1	6	0.23	-2	-1
F	Rib height	160	0.35	0	2	0.23	1	1
G	Rib width	80	0.84	2	8	0.2	0	1
I	Rebate depth	17	0.58	5	4	0.23	-3	-3
J	Rebate width	60	0.87	-3	-3	0.36	0	0
K1	Hole position	250	1.76	-3	2	0.3	-3	-2
K2	Hole position	250	0.87	3	5	0.36	1	2
M	Hole diameter	200	3.23	-40	-30	0.48	1	2

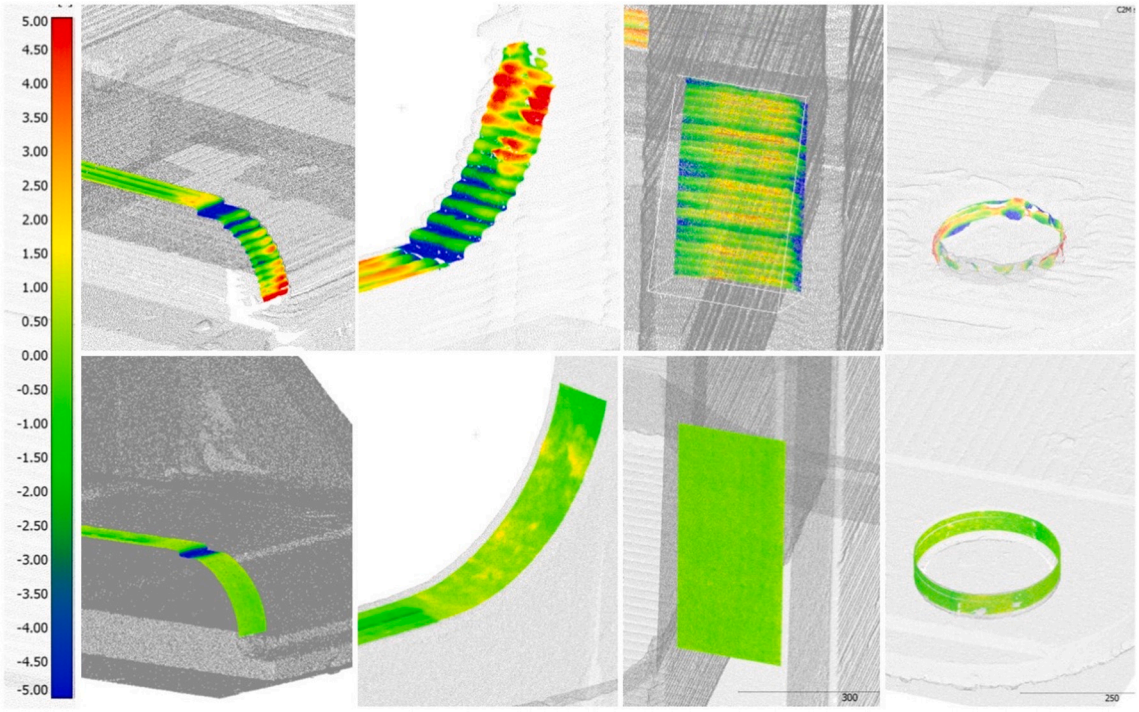

Fig. 9. Digitally augmented error inspection for the 3DCP and milled parts on features, rounded fillet, radius, flat surface, circular hole formation, photographed in Fig. 2. Errors (mm) are colour mapped on the left-hand scale.

systems, using the same reference geometry to drive the digital and mechanical processes to production. This captures all errors in the end-to-end production process, the impacts of which can then be measured in a standardised manner opening the way for systematic checks during commissioning and system optimisation procedures, through to comparing different technology instances, platforms and system architectures.

Through a standardised approach, it is hoped that benchmarking performance will be a possible way to enable routine and comparable statements about system performance to potential clients of the technology. In addition, the approach can be used to statistically evaluate production tolerances so that design for manufacture can be fully realised: this will become more important when designs are built on different systems through an increasingly globalised production network.

The test part is freely downloadable from [25] and this article is published as open access so that the standard measurement details are available for all to implement.

6.1. The benefits of hybrid manufacturing over 3DCP

The secondary milling does not automatically mean more accuracy. It requires a second set of modelling and tooling instructions and consequential robotic positional dependencies and hence there is more room for human error in the commissioning, design and execution of the tooling strategies. However, in terms of surface flatness and the precision of forming of edges, the hybrid method delivers to an exceptional degree, quite beyond what is possible with 3DCP alone as evidenced in Fig. 9, with surface flatness improved about four times. With more accurate commissioning of the positioning system, it is quite likely that Hybrid has the potential to achieve if not exceed the performance of traditional moulding techniques, as well as opening up other benefits as reported for other materials in different sectors [57–59].

6.2. Limitations of the test part approach

We endeavoured to capture a number of important geometrical features in the design of the test part, while minimising the build complexity so that most 3D concrete printers can make it. We restricted the design to two key elements found in the built environment, a panel and a wall section, and we augmented these with some useful but challenging features to reproduce in order to test accuracy and precision of processes.

We selected the reproduction of 90° edges and flat straight surfaces because these are challenging to reproduce for 3DCP and hence offer a tough target with which to evaluate against. These features have additional benefits, namely they are easy to evaluate using conventional, industry standard measurements and they are also very sensitive to errors, which makes issues easy to spot though visual inspection.

There were some omissions in the feature design. Curvature was limited to radiused vertices and cantilevers were excluded in order to maintain ease of measurement and simplicity of build. In addition, we acknowledge that for different process implementations and target applications, the filament size in particular can vary [2,30]. As filament bead and build scale increase, the dimensions of this part and the resolution of the features are likely to become less relevant. What is important is, that for a specific system, the test method used needs to engage all machine axes over their likely working range. This is a requisite for testing procedures so that quality can be assured within the whole machine build volume: it is particularly important for robotic positioning systems as position errors are unlikely to remain constant over the build area. In our instance, we limited the part to 1 m^3, which is a useful scale and all positional axis on our machine needed to be engaged in the part manufacture.

We focused on geometric analysis here, but extensions to the analysis of the digital data could evaluate the quality of repeatable features and variability of bead geometry amongst others. Cost of production is an important factor, however, production of a part at some point in commissioning a system will be required to verify the process: so why not use the same part as others and have the additional feedback that

standardised cross-platform benchmarking gives as value added?

6.3. Achieving accurate parts in practice

In this work, we took a very honest first pass approach at production. Clearly with future build iterations and armed with the information reported here, we would expect to get considerable improvements on both 3DCP and hybrid part accuracy. One of the most significant obstacles that we experienced on our system was the positioning accuracy of the robotic arm and in particular the synchronisation of that positioning with our turntable, which was needed to mill the far side of the part.

Metering at absolute distance with robotic arms is not something that robots are designed to do, and more work is needed to ensure better calibration of systems, or at least verification of acceptable accuracy. What was also evident was that when we were trying to produce a flat smooth surface, the position of the tooling becomes much more critical as errors are far more easily recognisable. However, the evidence is quite clear that the additional overhead of the preparation and tooling required to deliver the milling will deliver at least an order of magnitude greater accuracy and precision of the part, which is likely to be significant when 3DCP components of being integrated with each other and with other construction systems.

6.4. Measuring large parts

Measuring large components is challenging and accurate measurement with point cloud based-systems relies heavily on calibration procedures. The structured light approach used here with appropriately sized calibration boards enabled very high precision in our measurements: coverage of one point every 0.07 mm, with a point uncertainty of 0.45 mm.

The two-stage evaluation approach allows industry-standard methods to be used (visual inspection and linear dimensions by hand measurement) as well as greater depth of evaluation through application of digital techniques and analysis of point cloud data: automation of data capture and linear dimension evaluation, statistical measures of surface condition and digitally augmented visual analysis of complex features.

6.5. Outlook for quality control and assurance

A standardised geometry offers significant added value to the manufacture of test parts designed to exercise and verify a 3DCP or hybrid system. It can be used in one of a number of ways:

1) *Benchmark system capability*: to verify that the system has achieved certain stage of maturity, but also, as presented in this article, as part of that commissioning process to help diagnose problems and to promote improvements in system performance.
2) *Inter-process comparison*: if the part can be produced on one machine, then it can be compared to one produced on another, which is another powerful tool to improve the value added by the technology. This is important for system checking for machine providers and installers, but also to those investing to understand the comparative strengths of competing technologies. It allows alignment of capability across multiple installations by a manufacturer assuring product quality across its production sites. For technology developers, benchmarking performance against others will help increase the capability of their system offering.
3) *Quality monitoring*: the part can also be used for periodic checking for drift in manufacturing tolerances using interval-based testing which is a standard quality control procedure in manufacturing. In particular, where there has been a change in materials or process, such as servicing in production, using a part to verify manufacturing tolerance is important to check operations before production restarts.
4) *Development of processes*: benchmarking also brings a systematic approach evaluating the influence of process parameters and material performance for improving material deposition control and part formation during printing and for the development of secondary shaping and finishing processes to augment 3DCP.
5) *Evaluation of design tolerances*: critically through multiple production of the part, statistical measures of manufacturing tolerances can be determined and these underpin design for manufacture and integration with other construction systems. Understanding what geometries and features can be manufactured to what tolerance and to what level of confidence is a critical next step for the technology. With this comes the ability to minimise material while maintaining critical cross-sections in structures, it determines how accurately parts can interface with other building structures as well as underpinning the aesthetics of assemblies such as façades.

7. Conclusions

One of the main goals of the project that funded this work was to develop the ‘world’s most accurate 3-D printing process’ using a hybrid manufacturing approach. In the course of this endeavour, we realised that we are not in a position to make such a claim because we simply do not know how accurate or precise the concrete printing processes that are already in existence, but more than that, we have no way of comparing performance: until now.

With this freely available test part [25] and the measurement procedures outlined in this article, there is now a benchmark that can be replicated and measured on any 3-D printing system with a set of data to directly compare performance. The authors hope that this will be used by others and so open up the dialogue around geometric quality and then factors that influence it. Through constructive and well-motivated competition between actors in the academic and commercial communities, we hope that the level of precision achievable with 3DCP only and hybrid processes will rise to a level where it routinely exceeds what is cost effectively achievable using conventional manufacturing processes and in so doing, add significant value to the technology as it continues to make an impact on manufacture in architecture, construction, and infrastructure.

Declaration of competing interest

The authors declare that they have no known competing financial interests or personal relationships that could have appeared to influence the work reported in this paper.

Acknowledgements

This work was supported by the UK's Industrial Strategy Challenge Fund for Transforming Construction, UKRI grant number EP/S031405/1 and EP/S019618/1.

Appendix A

Table A.1
Summary of 3DCP products of which the form accuracy has been reported or evaluated.

Product		Bead width (BW) / Layer height (LH)	Reported form accuracy					Improvement treatment	Measurement methods	Product number
			Dimensional precision			Geometric accuracy				
			Lateral deviation	Z height deviation	Global profile deviation	Edge profile deviation	Texture position offset			
Single components	Wall & column	BW 8–120 mm (layer height to bead width ratio: 0.08–0.6)	≤+15.3 mm						Industrial cameras (imaging system)	2
					[−10 mm, +10 mm]			Post smoothing / milling	3D laser scanning / multi-view photogram-metry	6
			[−15 mm, +15 mm]						Laser scanning	8
	Cladding panel				Dome: [−5 mm, +5 mm] Saddle: [−9 mm, +9 mm]				Laser scanning	14
	Volumetric part (test specimen)			[−20 mm, +50 mm]					3D laser scanning	15
					[−59% BW, +84% BW]	External edge: [−104% BW, 0] Internal edge: [0, +163% BW]			Structured light scanning	16
Assembled structure	Pavilion (volumetric)				Half of the surface: ≥ 12 mm			3D laser scanning / Photogrammetry		21
Surface textures							[−6 mm, +6 mm]	Post profiling/ trowelling	Not given	23

Table A.2
Summary of 3DCP products of which the surface finish has been reported or evaluated.

Product		Bead width (BW) / Layer height (LH)	Reported surface finish							Improvement treatment	Measurement methods	Product number
			Waviness				Roughness					
			Vertical face flatness	Horizontal face flatness	Inclined face flatness	Curved surface waviness	Printed surface	Other surfaces	Void ratio			
Single components	Dome / vault (shell)					[−12 mm, +12 mm]	~1000 um				Microscribe 3DLX digitizer	9
	Volumetric part (test specimen)	BW 8–120 mm (layer height to bead width ratio: 0.08–0.6)	43–76% BW	44–49% BW	55–80% BW						Structured light scanning	16
			Rectangle nozzle: [−2.5 mm, 2 mm] Variable nozzle: [−1.7 mm, +0.8 mm]							Nozzle shape control	Not given	17
					Rectangle nozzle: [−4 mm, +3.5 mm] Variable nozzle: [−2 mm, +2 mm]					Nozzle shape control	Not given	18
						Concave: Rectangle				Nozzle shape control	Not given	19

(*continued on next page*)

Table A.2 (*continued*)

Product	Bead width (BW) / Layer height (LH)	Reported surface finish							Improvement treatment	Measurement methods	Product number
		Waviness				Roughness					
		Vertical face flatness	Horizontal face flatness	Inclined face flatness	Curved surface waviness	Printed surface	Other surfaces	Void ratio			
					nozzle: [−3 mm, +2.5 mm] Variable nozzle: [−2.5 mm, +2 mm] Convex (arch): Rectangle nozzle: [−4 mm, +4 mm] Variable nozzle: [−2 mm, +1 mm]				Nozzle shape control	Not given	20
Surface textures					(−3 mm, +3 mm)			>1.0%	Post profiling/ trowelling	Not given	23

References

[1] R.A. Buswell, W.R. Leal da Silva, F.P. Bos, H.R. Schipper, D. Lowke, N. Hack, H. Kloft, V. Mechtcherine, T. Wangler, N. Roussel, A process classification framework for defining and describing Digital Fabrication with Concrete, Cem. Concr. Res. 134 (2020), 106068, https://doi.org/10.1016/j.cemconres.2020.106068.

[2] G. Ma, R.A. Buswell, W.R. Leal da Silva, L. Wang, J. Xu, S.Z. Jones, Technology readiness: a global snapshot of 3D concrete printing and the frontiers for development, Cem. Concr. Res. 156 (2022) 106774, https://doi.org/10.1016/j.cemconres.2022.106774.

[3] I. Gibson, D. Rosen, B. Stucker, Additive Manufacturing Technologies 3D Printing, Rapid Prototyping, And Direct Digital Manufacturing, Springer, New York, NY, 2015, https://doi.org/10.1007/978-1-4939-2113-3.

[4] J. Xu, R.A. Buswell, P. Kinnell, I. Biro, J. Hodgson, N. Konstantinidis, L. Ding, Inspecting manufacturing precision of 3D printed concrete parts based on geometric dimensioning and tolerancing, Autom. Constr. 117 (2020), 103233, https://doi.org/10.1016/j.autcon.2020.103233.

[5] R.A. Buswell, P. Kinnell, J. Xu, N. Hack, H. Kloft, M. Maboudi, M. Gerke, P. Massin, G. Grasser, R. Wolfs, F. Bos, Inspection methods for 3D concrete printing, in: RILEM International Conference on Concrete And Digital Fabrication, Springer, Cham, 2020, July, pp. 790–803, https://doi.org/10.1007/978-3-030-49916-7_78.

[6] N. Hack, H. Kloft, Shotcrete 3d printing technology for the fabrication of slender fully reinforced freeform concrete elements with high surface quality: a real-scale demonstrator, in: RILEM International Conference on Concrete And Digital Fabrication, Springer, Cham, 2020, July, pp. 1128–1137, https://doi.org/10.1007/978-3-030-49916-7_107.

[7] W. Lao, M. Li, T.N. Wong, M.J. Tan, T. Tjahjowidodo, Improving surface finish quality in extrusion-based 3D concrete printing using machine learning-based extrudate geometry control, Virtual Phys. Prototyp. 15 (2) (2020) 178–193, https://doi.org/10.1080/17452759.2020.1713580.

[8] W. Lao, M. Li, T. Tjahjowidodo, Variable-geometry nozzle for surface quality enhancement in 3D concrete printing, Addit.Manuf. 37 (2021), 101638, https://doi.org/10.1016/j.addma.2020.101638.

[9] A. Anton, L. Reiter, T. Wangler, V. Frangez, R.J. Flatt, B. Dillenburger, A 3D concrete printing prefabrication platform for bespoke columns, Autom. Constr. 122 (2021), 103467, https://doi.org/10.1016/j.autcon.2020.103467.

[10] R.J. Wolfs, F.P. Bos, T.A.M. Salet, Early age mechanical behaviour of 3D printed concrete: numerical modelling and experimental testing, Cem. Concr. Res. 106 (2018) 103–116, https://doi.org/10.1016/j.cemconres.2018.02.001.

[11] S. Lim, R.A. Buswell, T. Le, R. Wackrow, S.A. Austin, A. Gibb, T. Thorpe, Development of a viable concrete printing process, in: 28th International Symposium on Automation And Robotics in Construction (ISARC2011), 29 Jun - 2 Jul 2011, Seoul, South Korea, 2011, pp. 665–670, https://doi.org/10.22260/ISARC2011/0124.

[12] G.M. Moelich, J. Kruger, R. Combrinck, Plastic shrinkage cracking in 3D printed concrete, Compos. Part B 200 (2020), 108313, https://doi.org/10.1016/j.compositesb.2020.108313.

[13] J. Bard, D. Cupkova, N. Washburn, G. Zeglin, Robotic concrete surface finishing: a moldless approach to creating thermally tuned surface geometry for architectural building components using profile-3D-printing, Constr.Robot. 2 (1–4) (2018) 53–65, https://doi.org/10.1007/s41693-018-0014-x.

[14] H. Lindemann, R. Gerbers, S. Ibrahim, F. Dietrich, E. Herrmann, K. Dröder, A. Raatz, H. Kloft, Development of a shotcrete 3D-printing (SC3DP) technology for additive manufacturing of reinforced freeform concrete structures, in: RILEM International Conference on Concrete And Digital Fabrication, Springer, Cham, 2018, September, pp. 287–298, https://doi.org/10.1007/978-3-319-99519-9_27.

[15] M.M. Muñiz, M. Chantin, C.R. Vintila, M. Fabritius, C. Martin, L. Calvo, L. Poudelet, J. Canou, M. Uhart, A. Papacharalampopoulos, P. Stavropoulos, Concrete hybrid manufacturing: a machine architecture, Procedia CIRP 97 (2021) 51–58, https://doi.org/10.1016/j.procir.2020.07.003.

[16] J. Dobrzanski, R.A. Buswell, S. Cavalaro, P. Kinnell, W. Wang, J. Xu, J. Kolawole, Milling a cement-based 3D printable mortar in its green state using a ball-nosed cutter, Cem. Concr. Compos. 125 (2022), 104266, https://doi.org/10.1016/j.cemconcomp.2021.104266.

[17] E.P. Gargiulo, D. Belfiore, Stereolithography process accuracy: user experience, in: Proceedings of the 1st European Conference on Rapid Prototyping, University of Nottingham, 1992, July, pp. 187–207.

[18] M. Mahesh, Y.S. Wong, J.Y.H. Fuh, H.T. Loh, Benchmarking for comparative evaluation of RP systems and processes, Rapid Prototyp. J. (2004), https://doi.org/10.1108/13552540410526999.

[19] J.P. Kruth, B. Vandenbroucke, J. Van Vaerenbergh, P. Mercelis, Benchmarking of different SLS/SLM processes as rapid manufacturing techniques, in: Proceedings of the International Conference Polymers & Moulds Innovations PMI 2005, 2005.

[20] L. Castillo, Study about the rapid manufacturing of complex parts of stainless steel and titanium, in: TNO Report With the Collaboration of AIMME, 2005, pp. 1–31.

[21] G.D. Kim, Y.T. Oh, A benchmark study on rapid prototyping processes and machines: quantitative comparisons of mechanical properties, accuracy, roughness, speed, and material cost, Proc. Inst. Mech. Eng. B J. Eng. Manuf. 222 (2) (2008) 201–215, https://doi.org/10.1243/09544054JEM724.

[22] T.A. Grimm, 3D Printer Benchmark, North American Edition, TA Grimm & Associates Inc, 2010 www. tagrimm. com.

[23] S. Moylan, J. Slotwinski, A. Cooke, K. Jurrens, M.A. Donmez, Proposal for a standardized test artifact for additive manufacturing machines and processes, in: Proceedings of the 2012 Annual International Solid Freeform Fabrication Symposium, 2012, August, pp. 6–8. Austin, TX.

[24] Y.L. Yap, C. Wang, S.L. Sing, V. Dikshit, W.Y. Yeong, J. Wei, Material jetting additive manufacturing: an experimental study using designed metrological benchmarks, Precis. Eng. 50 (2017) 275–285, https://doi.org/10.1016/j.precisioneng.2017.05.015.

[25] D. Becker, J. Dobrzanski, J. Xu, P. Kinnell, J. Provis, R.A. Buswell, CAD model of a standardised test geometry for benchmarking 3D Concrete Printing and hybrid construction manufacturing system capability, Loughborough University, 2022. Online resource, https://doi.org/10.17028/rd.lboro.19165919.

[26] Wohlers, Wohlers Report 2021: 3D Printing And Additive Manufacturing, Global State of the Industry, Wohlers Associates, Colorado, USA, 2021.

[27] L.E. Thomas-Seale, J.C. Kirkman-Brown, M.M. Attallah, D.M. Espino, D. E. Shepherd, The barriers to the progression of additive manufacture: Perspectives from UK industry, Int. J. Prod. Econ. 198 (2018) 104–118, https://doi.org/10.1016/j.ijpe.2018.02.003.

[28] R. Lezama-Nicolás, M. Rodríguez-Salvador, R. Río-Belver, I. Bildosola, A bibliometric method for assessing technological maturity: the case of additive manufacturing, Scientometrics 117 (3) (2018) 1425–1452, https://doi.org/10.1007/s11192-018-2941-1.

[29] R. Hague, P. Reeves, S. Jones, 'Mapping UK research and innovation in additive manufacturing: A review of the UK's publicly funded R&D activities in additive manufacturing between 2012 and 2015'. Report commissioned and published by Innovate UK, in collaboration with the EPSRC Centre for Innovative Manufacturing in Additive Manufacturing, and carried out by Stratasys Strategic Consulting (formerly Econolyst Ltd), 2016.
[30] F.P. Bos, C. Menna, M. Pradena, E. Kreiger, W.R. Leal da Silva, A.U. Rehman, D. Weger, R.J.M. Wolfs, Y. Zhang, L. Ferrara, V. Mechtcherine, The realities of additively manufactured concrete structures in practice, Cem. Concr. Res. 156 (2022) 106746, https://doi.org/10.1016/j.cemconres.2022.106746.
[31] A. Nassehi, S. Newman, V. Dhokia, Z. Zhu, R.I. Asrai, Using formal methods to model hybrid manufacturing processes, in: Enabling Manufacturing Competitiveness And Economic Sustainability: Proceedings of the 4th International Conference on Changeable, Agile, Reconfigurable and Virtual production (CARV2011), Montreal, Canada, 2-5 October 2011, Springer Science & Business Media, 2011, September, p. 52.
[32] T. Tawakoli, B. Azarhoushang, Influence of ultrasonic vibrations on dry grinding of soft steel, Int. J. Mach. Tools Manuf. 48 (14) (2008) 1585–1591, https://doi.org/10.1016/j.ijmachtools.2008.05.010.
[33] R. Kolleck, R. Vollmer, R. Veit, Investigation of a combined micro-forming and punching process for the realization of tight geometrical tolerances of conically formed hole patterns, CIRP Ann. 60 (1) (2011) 331–334, https://doi.org/10.1016/j.cirp.2011.03.141.
[34] CIRP, CIRP - the internal academy for production engineering [online], Available from, www.cirp.net, 2011.
[35] S. Keating, N.A. Spielberg, J. Klein, N. Oxman, A compound arm approach to digital construction, in: Robotic Fabrication in Architecture, Art And Design 2014, Springer, Cham, 2014, pp. 99–110, https://doi.org/10.1007/978-3-319-04663-1_7.
[36] J. Canou, M. Uhart, D.I.A.Z. Pierre, A "low-cost" subtractive method for freshly finished 3D concrete printed structures, Procedia Comput.Sci. 180 (2021) 32–39, https://doi.org/10.1016/j.procs.2021.01.125.
[37] S.J. Keating, J.C. Leland, L. Cai, N. Oxman, Toward site-specific and self-sufficient robotic fabrication on architectural scales, Sci.Robot. 2 (5) (2017), https://doi.org/10.1126/scirobotics.aam8986.
[38] P. Carneau, R. Mesnil, N. Roussel, O. Baverel, Additive manufacturing of cantilever-from masonry to concrete 3D printing, Autom. Constr. 116 (2020), 103184, https://doi.org/10.1016/j.autcon.2020.103184.
[39] S. Lim, R.A. Buswell, P.J. Valentine, D. Piker, S.A. Austin, X. De Kestelier, Modelling curved-layered printing paths for fabricating large-scale construction components, Addit.Manuf. 12 (2016) 216–230, https://doi.org/10.1016/j.addma.2016.06.004.
[40] C.B. Costanzi, Z.Y. Ahmed, H.R. Schipper, F.P. Bos, U. Knaack, R.J.M. Wolfs, 3D printing concrete on temporary surfaces: the design and fabrication of a concrete shell structure, Autom. Constr. 94 (2018) 395–404, https://doi.org/10.1016/j.autcon.2018.06.013.
[41] Z. Ahmed, A. Biffi, L. Hass, F. Bos, T. Salet, 3D concrete printing-free form geometries with improved ductility and strength, in: RILEM International Conference on Concrete And Digital Fabrication, Springer, Cham, 2020, July, pp. 741–756, https://doi.org/10.1007/978-3-030-49916-7_74.
[42] J.H. Lim, Y. Weng, Q.C. Pham, 3D printing of curved concrete surfaces using Adaptable Membrane Formwork, Constr. Build. Mater. 232 (2020), 117075, https://doi.org/10.1016/j.conbuildmat.2019.117075.
[43] G. Grasser, L. Pammer, H. Köll, E. Werner, F.P. Bos, Complex architecture in printed concrete: the case of the Innsbruck University 350 th Anniversary Pavilion COHESION, in: RILEM International Conference on Concrete And Digital Fabrication, Springer, Cham, 2020, July, pp. 1116–1127, https://doi.org/10.1007/978-3-030-49916-7_106.
[44] C.A. Battaglia, M.F. Miller, K.P. Verian, Print-cast concrete: additive manufacturing for 3D printing mortar in robotically fabricated green sand molds, in: RILEM International Conference on Concrete And Digital Fabrication, Springer, Cham, 2020, July, pp. 757–767, https://doi.org/10.1007/978-3-030-49916-7_75.
[45] J. Xu, L. Ding, L. Cai, L. Zhang, H. Luo, W. Qin, Volume-forming 3D concrete printing using a variable-size square nozzle, Autom. Constr. 104 (2019) 95–106, https://doi.org/10.1016/j.autcon.2019.03.008.
[46] C. Gosselin, R. Duballet, P. Roux, N. Gaudillière, J. Dirrenberger, P. Morel, Large-scale 3D printing of ultra-high performance concrete–a new processing route for architects and builders, Mater. Des. 100 (2016) 102–109, https://doi.org/10.1016/j.matdes.2016.03.097.
[47] N. Gaudillière, R. Duballet, C. Bouyssou, A. Mallet, P. Roux, M. Zakeri, J. Dirrenberger, Large-scale additive manufacturing of ultra-high-performance concrete of integrated formwork for truss-shaped pillars, in: Robotic Fabrication in Architecture, Art And Design, Springer, Cham, 2018, September, pp. 459–472, https://doi.org/10.1007/978-3-319-92294-2_35.
[48] T.T. Le, S.A. Austin, S. Lim, R.A. Buswell, A.G. Gibb, T. Thorpe, Mix design and fresh properties for high-performance printing concrete, Mater. Struct. 45 (8) (2012) 1221–1232, https://doi.org/10.1617/s11527-012-9828-z.
[49] T.T. Le, S.A. Austin, S. Lim, R.A. Buswell, R. Law, A.G. Gibb, T. Thorpe, Hardened properties of high-performance printing concrete, Cem. Concr. Res. 42 (3) (2012) 558–566, https://doi.org/10.1016/j.cemconres.2011.12.003.
[50] J.T. Kolawole, R. Combrinck, W.P. Boshoff, Shear rheo-viscoelasticity approach to the plastic cracking of early-age concrete, Cem. Concr. Res. 135 (2020), 106127, https://doi.org/10.1016/j.cemconres.2020.106127.
[51] D. Lootens, P. Jousset, L. Martinie, N. Roussel, R.J. Flatt, Yield stress during setting of cement pastes from penetration tests, Cem. Concr. Res. 39 (5) (2009) 401–408, https://doi.org/10.1016/j.cemconres.2009.01.012.
[52] CloudCompare - 3D point cloud and mesh processing software Open Source Project. https://www.danielgm.net/cc/ last accessed on 01/02/2022.
[53] R.A. Buswell, F.P. Bos, W.R.Leal da Silva, N. Hack, H. Kloft, D. Lowke, N. Freund, A. Fromm, E. Dini, T. Wangler, E. Lloret-Fritschi, R. Schipper, V. Mechtcherine, A. Perrot, K. Vasilic, N. Roussel, Digital fabrication with cement-based materials: process classification and case studies, in: N. Roussel, D. Lowke (Eds.), Digital Fabrication With Cement-based Materials. RILEM State-of-the-Art Reports vol. 36, Springer, Cham, 2022, https://doi.org/10.1007/978-3-030-90535-4_2.
[54] A. de la Fuente, A. Blanco, E. Galeote, S. Cavalaro, A structural fibre-reinforced cement-based composite oriented to particle bed 3D-printing systems. Case study: Parque de Castilla (Alcobendas, Madrid) Footbridge, Cem. Concr. Res. 157 (2022), 106801.
[55] N. Roussel, R.A. Buswell, N. Ducoulombier, I. Ivanova, J. Kolawole, D. Lowke, V. Mechtcherine, R. Mesnil, A. Perrot, U. Pott, L. Reiter, D. Stephan, T. Wangler, R. Wolfs, W. Zuo, Rheology assessment of printable materials: requirements and potential testing methods, in: Cement And Concrete Research: SI Digital Concrete DC2022, 2022. XXXXXXXXXXXXXXXXXX.
[56] V. Mechtcherine, K. Tittelboom, A. Kazemian, E. Kreiger, B. Nematollahi, V. N. Narella, M. Santhanam, G. de Schutter, G.V. Zijl, D. Lowke, E. Ivaniuk, M. Taubert, F. Bos, A road map for quality control of hardening and hardened printed concrete, Cem. Concr. Res. 157 (2022), 106800.
[57] M. Merklein, D. Junker, A. Schaub, F. Neubauer, Hybrid additive manufacturing technologies–an analysis regarding potentials and applications, Phys. Procedia 83 (2016) 549–559, https://doi.org/10.1016/j.phpro.2016.08.057.
[58] J.M. Flynn, A. Shokrani, S.T. Newman, V. Dhokia, Hybrid additive and subtractive machine tools–research and industrial developments, Int. J. Mach. Tools Manuf. 101 (2016) 79–101, https://doi.org/10.1016/j.ijmachtools.2015.11.007.
[59] L. Li, A. Haghighi, Y. Yang, A novel 6-axis hybrid additive-subtractive manufacturing process: design and case studies, J. Manuf. Process. 33 (2018) 150–160, https://doi.org/10.1016/j.jmapro.2018.05.008.